frontiers | Frontiers in Applied Mathematics and Statistics

TYPE Original Research
PUBLISHED 19 December 2023
DOI 10.3389/fams.2023.1282544

OPEN ACCESS

EDITED BY
Hagos Hailu Gidey,
Botswana International University of Science and Technology, Botswana

REVIEWED BY
Adebayo Aderogba,
Obafemi Awolowo University, Nigeria
Sania Qureshi,
Mehran University of Engineering and Technology, Pakistan

*CORRESPONDENCE
Jemal Muhammed Ahmed
✉ jemalmuhammed332@gmail.com

RECEIVED 24 August 2023
ACCEPTED 27 November 2023
PUBLISHED 19 December 2023

CITATION
Ahmed JM, Tilahun GT and Degefa ST (2023) A cell-level dynamical model for malaria parasite infection with antimalarial drug treatment. *Front. Appl. Math. Stat.* 9:1282544. doi: 10.3389/fams.2023.1282544

A cell-level dynamical model for malaria parasite infection with antimalarial drug treatment

Jemal Muhammed Ahmed[1]*, Getachew Teshome Tilahun[2] and Shambel Tadesse Degefa[1]

[1]Department of Applied Mathematics, Adama Science and Technology University, Adama, Ethiopia, [2]Department of Mathematics, Haramaya University, Haramaya, Ethiopia

Malaria is an infectious disease caused by intracellular parasites of the genus Plasmodium. It is a major health problem around the world. In this study, a cell-level mathematical model of malaria parasites with antimalarial drug treatments is formulated and analyzed. The model consists of seven compartments for cell populations. We analyzed the qualitative behavior of the model using various techniques. The stability analysis of the parasite-free equilibrium is obtained, whereas it is locally and globally stable if the basic reproduction number $\mathcal{R}_0 < 1$. The parasite persistence equilibrium point exists, and it is locally asymptotically stable if $\mathcal{R}_0 > 1$. The sensitivity analysis of the basic reproduction number is computed, and the results show that the infection rate of the erythrocyte by merozoites, the average number of merozoites per ruptured infected erythrocyte cells, the natural death rate of merozoites, and the requirement rate of the uninfected erythrocyte are the most influential parameters within-host dynamics of malaria infection. Different numerical simulations are performed to supplement our analytical findings. The effect of primary tissue schizontocides, blood schizontocides, and gametocytocides on infected hepatocytes, infected erythrocytes, and gametocytes have been investigated, respectively. Finally, some counterplots are presented in order to investigate the impact of parameters on the basic reproduction number. The in-host basic reproduction number decreases as the antimalarial treatment administration increases. Therefore, increasing antimalarial treatment administration is the best way to mitigate the in-host malaria infection.

KEYWORDS

blood schizontocides, gametocytocides, dynamical system, sensitivity analysis, erythrocytes, hepatocytes

1 Introduction

Malaria still poses a danger to global health as well as affects economic growth and progress in high-burden areas. Nearly half of the world population is at risk for malaria infection, with approximately half a million deaths per year [1, 2], mainly in African countries, among children under 5 years of age [3]. Malaria is caused by intracellular parasites of the genus *Plasmodium*; of these, *Plasmodium falciparum* is the most virulent form among the five species (*P. vivax, P. ovale, P. malaria, P. falciparum*, and *P. knowlesi*) that infect humans [4]. Malaria is a life-threatening disease that is transmitted between humans via vectors (during the blood meal of female Anglophile mosquitoes).

Malaria infection begins when malaria parasites in the form of sporozoites are deposited by female Anopheles mosquitoes into the host's skin during a blood meal. After a short period of time, the sporozoites travel to the liver. The liver-stage of Plasmodium infection

is required and occurs when mosquito-transmitted Plasmodium sporozoites infiltrate hepatocytes [5]. This stage is clinically silent and untreatable, and affected individuals are asymptomatic. Inside the hepatocyte, a parasite divides into thousands of merozoites through a process called schizogony, where they differentiate into pre-erythrocytic forms (PEFs) [6]. The matured infected liver (schizont) ruptures and releases thousands of merozoites into the bloodstream, invading red-blood cells (RBCs) [7].

The infected red-blood cells developed through the ring, trophozoites, and schizont phases [8]. The parasite remains in its ring form, which has low morphological change and limited metabolic activity. The parasite then progresses to the mature trophozoite (feeding) stage, where it develops quickly and becomes more metabolically active. The parasite eventually transforms into a schizont with the commencement of nuclear division [9], and the resulting mature schizont contains 16–32 daughter merozoites. These schizonts ruptured, releasing daughter merozoites to invade new RBCs. This cycle of erythrocytic development depends on the parasite species [8, 9], and it is during this stage that an individual will start to experience malaria-related symptoms such as periodic fever upon each bursting phase of the infected red-blood cells to release the merozoites. The fever decreases during the parasite replicating phase inside the RBCs, and the patient appears to be improving [10].

A certain amount of merozoites develop into sexual gametocytes within the host in the form of male (microgametes) and female (macrogametes) gametocytes in the infected red-blood cells. The mosquito ingested these gametocytes while feeding on blood. In the mosquito's gut, the male and female gametocytes join to produce a zygote [11], which grows into an ookinete and migrates through the midgut epithelium of the mosquito to become an oocyst between 24 and 36h later. The oocyst then develops into sporozoites through asexual sporogenic replication [12–16]. The WHO suggests using combination therapy against parasites in the asexual hepatocytic, and erythrocytic stages that has been associated with clinical symptoms and the accompanying mortality. The development of vaccinations, vector control, chemotherapy with antimalarial medications, chemoprophylaxis, and other methods are the primary ways that malaria is eliminated or reduced in prevalence. Most antimalarials act by targeting two or more phases of the parasite's life cycle in order to prevent it [17].

The antimalarial therapies have been developed and classified as *primary tissue schizontocides* act on the pre-erythrocytic forms (primary tissue phases) of the malaria parasite. Administration of medications that destroy sporozoites or the primary tissue forms entirely avoids erythrocytic infection. The primaquine and pamaquine are active in the primary tissue schizonts. Additionally, metformin therapy inhibits *Plasmodium falciparum* development in human hepatocytes, which may result in pretreatment-induced defects in parasite invasion or effective clearance of liver-stage Plasmodium parasites [18]. *Blood schizontocides* act on the asexual erythrocytic forms of all malaria parasites. Quinine, mepacrine, 4-aminoquinolines, and chloroquine are used to treat and effectively reduce blood schizonts due to their powerful and quick actions [19]. *Gametocytocidal drugs (gametocytocides)* prevent the transmission of parasites into mosquitoes and reduce the human reservoir of the disease. The 8-aminoquinolines, pamaquine, plasmocide, primaquine, and quinocide are most active in the sexual forms of all species of malaria parasites [20].

Although most of the time, artemisinin-based combination therapies (ACT) are recommended by the WHO to treat malaria with Plasmodium, such as artemether plus lumefantrine, artesunate plus amodiaquine, artesunate plus mefloquine, dihydroartemisinin plus piperaquine, artesunate plus sulfadoxine–pyrimethamine (SP), artesunate plus tetracycline or doxycycline or clindamycin, and quinine plus tetracycline or doxycycline or clindamycin [21], which are recommended for uncomplicated malaria infection [22].

Several mathematical malaria models have been developed and studied at in-host levels, with important results toward the evolution of malaria, Plasmodium. Anderson et al. [23] developed a within-host model. The authors analyzed non-linear dynamical phenomena in host-parasite interactions with reference to a series of different problems ranging from the impact on the transmission of control measures based on vaccination and chemotherapy to the effects of immunologic responses targeted at different stages in a parasite's life cycle. Hetzel and Anderson [24] discovered the blood-stage malaria parasite in the absence of a human immune response. They consider the densities of three cell populations: healthy red-blood cells, infected red-blood cells, and free merozoites. Elaiw and Agha [25] studied a reaction-diffusion model for the blood-stage dynamics of malaria infection with CTL and antibody immune responses. The model explores the interactions between uninfected red-blood cells (erythrocytes), three types of infected red-blood cells, free merozoites, CTLs, and antibodies. They introduced some parameters to measure the effect of antimalarial drugs and isoleucine starvation on the blood cycle of malaria infection.

In the study by Li et al. [26], the blood-stage dynamics of malaria in an infected human host including susceptible red-blood cells, infected red-blood cells, malaria parasitemia, and immune effectors, a mathematical model was discovered. The authors generalized from Anderson [27] and Anderson et al. [23] using non-linear bounded Michaelis-Menten-Monod functions to describe how the immune system interacts with the infected red-blood cells and merozoites. The model displayed that periodic oscillations occur as a result of Hopf bifurcation at the positive equilibrium, illuminating the fact that the immune response and malaria infections are always linked. Song et al. [28] investigated the two inside-the host mathematical models (with and without immune responses) for replicating the dynamics of the malaria parasites. The researchers also incorporate competition (between parasites that are drug-sensitive and those that are drug-resistant), drug treatment, and immunologic response whenever examining the evolution of drug resistance inside an infected host. The studies [29–33] are projected for the blood stage malaria parasites with immune response.

In a study by Tabo et al. [34], the interaction of the malaria parasite in sexual and asexualual stages during its life cycle, i.e., a combination of hepatocyte stage, erythrocyte stage, and mosquito-stage malaria parasite into one mathematical model is studied. The authors also include blood-stage treatment as a control strategy and investigate the effect of the treatment for malaria control within the host. The model that represents the dynamics of healthy hepatocytes, infected hepatocytes, sporozoites in the infected liver, healthy erythrocytes, infected erythrocytes, merozoites in

the blood, and gametocytes in the mosquito, and oocysts in the mosquito. The study [35] proposed the within-host dynamics of malaria infection with the immune system and treatment. The researchers considered the interactions of the hepatocyte cells, erythrocyte cells, malaria parasites, and immune cells. The findings indicated the progression of malaria and control of the disease with a treatment strategy that combines very efficient medications against malaria parasites with effective immune responses. The studies [34, 36, 37] are proposed the in-host dynamics of malaria infection by considering both erythrocyte stage and hepatocyte stage malaria infection. However, to the best of our knowledge, no study has considered the within-host dynamics of malaria parasites with stage-specific antimalarial drug treatment.

In this study, we investigated the within-host dynamics of malaria infection with primary liver-stage antimalarial drug treatment (tissue schizontocides), blood-stage antimalarial drug treatment (blood schizontocides), and gametocytocidal drug treatment (gametocytocides). We present the local and global stability of the parasite-free equilibrium point. It shows that the parasite-free equilibrium point is both local and global stable if basic reproduction is less than one. The existence and local stability analysis of the parasite-persistence equilibrium is shown. In addition, in order to supplement the theoretical and analytical results, we instantiate different numerical simulations. The rest of the study is organized as follows: In Section 2, the mathematical model is formulated. In Section 3, qualitative analysis of the model is investigated. Numerical simulation is performed in Section 4. The conclusion of the study is conferred in Section 5.

2 Model formulation

In this study, we provide a deterministic model that describes the inside-human-host dynamics of malaria Plasmodium. Our model contains seven compartments, as follows: uninfected hepatocyte $H(t)$, infected hepatocyte $H_I(t)$, uninfected RBCs $R(t)$, infected red-blood cell (iRBCs) $R_I(t)$, malaria parasite in the form of sporozoite $S(t)$, malaria parasite in the form of merozoite $M(t)$, and gametocyte $G(t)$ at time t.

The malaria parasite in the form of sporozoites is recruited from the salivary gland of the female Anopheles mosquito, with the blood meals at a constant rate π_S and die naturally at a rate μ_S. The hepatocyte cells are supplied from the bone marrow at a rate π_H. The hepatocytes are invaded by sporozoites that are injected into the human body during mosquito blood feeding at a constant rate β_1. This invasion is reduced due to tissue schizontocides (liver-stage antimalarial drug treatment) which is administrated pre-erythrocytic stage of malaria infection at a rate $(1-\xi_1)\beta_1$, where ξ_1 $(0 < \xi_1 \leq 1)$ is the efficacy of antimalarial drug on pre-erythrocytic malaria stage. The hepatocytes suffered natural death at a constant rate μ_H. The population of infected hepatocytes increases as the healthy hepatocytes get infection at a rate $(1-\xi_1)\beta_1$ and decreases owing to ruptured and die at a rate δ. The healthy erythrocytes (RBCs) are recruited from the bone marrow at a constant rate π_R. They acquire infection due to the invasion of merozoites that are released from the liver schizont at a rate β_2. The invasion rate is attenuated when blood-stage antimalarial drug treatment (blood-schizontocides) is administrated at the rate $(1-\xi_2)\beta_2$, where $\xi_2(0 < \xi_2 \leq 1)$ is the efficacy of antimalarial treatment on erythrocytic invasion, and the RBCs die naturally at a constant rate μ_R. The iRBCs burst and die at a constant rate σ. The merozoite population is produced when the infected hepatocyte ruptures and releases thousands of merozoites into the blood system at a rate δN, where N is the average number of merozoite released per ruptured infected hepatocytic cells, and during the iRBCs ruptured and release 16–32 merozoites per ruptured iRBC into the bloodstream at a constant rate σQ to invade fresh erythrocytes (RBCs), where Q is the average number of merozoites per ruptured iRBCs.

The production of the merozoite is reduced when antimalarial drug treatments; primary tissue(pre-erythrocytic) schizontocides and blood schizontocides are administrated at the rate of $(1-\xi_3)N$ and $(1-\xi_3)Q$, respectively, where $\xi_3(0 < \xi_3 \leq 1)$ is the efficacy of antimalarial drug treatments on the average number of merozoites rupturing rate of pre-erythrocytic schizont and blood schizont. The population of merozoite will reduce due to the natural death rate μ_M. After the invasion of the red-blood cells, some number of merozoites develop into male (microgametes) and female (macrogametes) gametocytes that arise within-host at a rate c. The sexual form (gametocytes) are destroyed due to the administration of gametocytocide [19] at a rate ξ_4 $(0 < \xi_4 \leq 1)$. The gametocytes die naturally at a rate μ_G. Note that, $\xi_i = 0$, $i = 1,\ldots,4$ implies that the antimalarial drug treatments are not effective at all, and $\xi_i = 1$ means that they are 100% effective. Assume that an uninfected erythrocyte's observation of merozoites and an uninfected hepatocyte's observation of sporozoites are ignored. The state variables and all the model biological parameters are listed in Tables 1, 2, respectively. Based on the above descriptions and the model schematic diagram (Figure 1), the formulated model equation is given by

$$\begin{aligned}
\frac{dH}{dt} &= \pi_H - (1-\xi_1)\beta_1 HS - \mu_H H,\\
\frac{dH_I}{dt} &= (1-\xi_1)\beta_1 HS - \delta H_I,\\
\frac{dR}{dt} &= \pi_R - (1-\xi_2)\beta_2 RM - \mu_R R,\\
\frac{dR_I}{dt} &= (1-\xi_2)\beta_2 RM - \sigma R_I,\\
\frac{dS}{dt} &= \pi_S - \mu_S S,\\
\frac{dM}{dt} &= (1-\xi_3)N\delta H_I + (1-\xi_3)Q\sigma R_I - \mu_M M,\\
\frac{dG}{dt} &= cR_I - \xi_4 G - \mu_G G,
\end{aligned} \tag{1}$$

with non-negative initial condition

$$\begin{aligned}
&H(0) = H_0, H_I(0) = H_{I0}, M(0) = M_0, S(0) = S_0, R(0) = R_0,\\
&R_I(0) = R_{I0}, G(0) = G_0.
\end{aligned} \tag{2}$$

3 Qualitative analysis of the model

In this section, we investigate the positivity and boundedness of the developed model, equilibria, stability analysis of the equilibria, and sensitivity analysis of basic reproduction number.

TABLE 1 State variables and their description.

State variables	Description
$H(t)$	Concentrations of the uninfected hepatocyte cells at time t
$H_I(t)$	Concentrations of the infected hepatocyte cells at time t
$S(t)$	Concentrations of the malaria parasite in the form of sporozoites at time t
$M(t)$	Concentrations of the malaria parasite in the form of merozoites at time t
$R(t)$	Concentrations of the uninfected erythrocyte cell at time t
$R_I(t)$	Concentrations of the infected erythrocyte cell at time t
$G(t)$	Concentrations of the malaria gametocytes at time t

TABLE 2 Model parameters and their description.

Parameters	Description
π_P	The recruitment rate of sporozoites from the salivary gland of the mosquito during blood meal
π_H	Production rate of the uninfected hepatocyte from the bone marrow
π_R	Production rate of the uninfected erythrocyte from the bone marrow
β_1	The infection rate of the hepatocyte by sporozoites
β_2	The infection rate of the erythrocyte by merozoites
δ	The death rate of the infected hepatocyte
N	The average number of merozoite per ruptured infected hepatocyte cells
Q	The average number of merozoite per ruptured infected erythrocyte cells
μ_H	The natural death rate of hepatocyte cells
μ_M	The natural death rate of merozoites
μ_P	The natural death rate of sporozoites
μ_R	The natural death rate of erythrocyte cells
σ	The death rate of infected erythrocyte cells
μ_G	The death rate of gametocyte
c	The rate of sexual replication of merozoites
ξ_1	Efficacy of antimalarial drugs on pre-erythrocytic malaria stage
ξ_2	Efficacy of antimalarial treatment for erythrocytic invasion
ξ_3	The efficiency of antimalarial drug treatments on the bursting rate of pre-erythrocytic schizont and blood schizont
ξ_4	The efficiency of gametocytocidal on the sexual development of the merozoites

3.1 Positivity and boundedness of the solution

Theorem 1. The solutions of system (Equation 1) with non-negative initial conditions, $H_0, H_{I0}, R_0, R_{I0}, M_0, S_0$, and G_0, remain non-negative for all time $t \geq 0$.

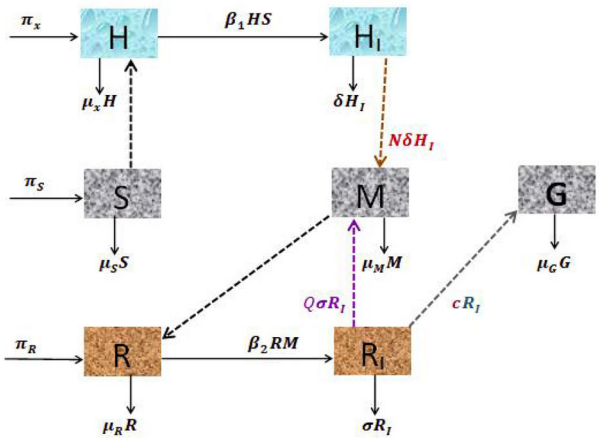

FIGURE 1
Schematic diagram of the dynamical system of hepatocytic-erythrocytic stage malaria parasite.

Proof 1. The first equation of dynamical system (Equation 1) gives rise to

$$\frac{dH}{dt} = \pi_H - (1-\xi_1)\beta_1 HS - \mu_H H \geq -((1-\xi_1)\beta_1 S + \mu_H)H,$$
$$\frac{dH}{H} \geq -((1-\xi_1)\beta_1 S + \mu_H)dt,$$
$$\int_0^t \frac{dH}{H} \geq -\int_0^t ((1-\xi_1)\beta_1 S + \mu_H)dt,$$
$$H(t) \geq H_0 e^{-\int_0^t ((1-\xi_1)\beta_1 S + \mu_H)dt} > 0.$$

The second equation of dynamical system (Equation 1) gives rise to

$$\frac{dH_I}{dt} = (1-\xi_1)\beta_1 HS - \delta H_I \geq -\delta H_I,$$
$$\frac{dH_I}{H_I} \geq -\delta dt, \quad \int_0^t \frac{dH_I}{H_I} \geq -\int_0^t \delta dt,$$
$$H_I(t) \geq H_{I0} e^{-\delta t} \geq 0.$$

In the same procedure, it can be shown that the state variables $R(t), R_I(t), S(t), M(t)$, and $G(t)$ are non-negative for all $t \geq 0$. Therefore, the solution of the dynamical system (Equation 1) is non-negative for all $t \geq 0$.

Theorem 2. The biologically feasible region

$$\Omega = \left\{(H, H_I, R, R_I, S, M, G) \in R_+^7 : N_H \leq \frac{\pi_H}{d_1}, N_R \leq \frac{\pi_R}{d_2} \text{ and } N_S \leq \frac{\pi_S}{d_3}\right\}$$

is positively invariant to the dynamical system (Equation 1).

Proof 2. The total hepatocyte population at a time t is denoted by $N_H(t)$ and defined as

$$N_H(t) = H(t) + H_I(t). \tag{3}$$

By differentiating (Equation 2) with respect to time t, we obtain

$$\begin{aligned}\frac{dN_H}{dt} &= \pi_H - (1-\xi_1)\beta_1 HS - \mu_H H + (1-\xi_1)\beta_1 HS - \delta H_I \\ &= \pi_H - \mu_H H - \delta H_I, \\ &\leq \pi_H - d_1 N_H, \ where \ d_1 = min\{\mu_H, \delta\}, \\ N_H(t) &\leq \frac{\pi_H}{d_1} + \left(N_{H0} - \frac{\pi_H}{d_1}\right) e^{-d_1 t}.\end{aligned} \tag{4}$$

Similarly, we can apply this procedure to red-blood cells $N_R(t) = R(t) + R_I(t)$.

$$\begin{aligned}&\frac{dN_R}{dt} = \pi_R - (1-\xi_2)\beta_2 RM - \mu_R R + (1-\xi_2)\beta_2 RM - \sigma R_I - cR_I, \\ &= \pi_R - \mu_R R - \sigma R_I \leq \pi_R - d_2 N_R, \quad where \ d_2 = min\{\mu_R, \sigma\}, \\ &N_R(t) \leq \frac{\pi_R}{d_2} + \left(N_{R0} - \frac{\pi_R}{\mu_{R'}}\right) e^{-d_2 t}.\end{aligned} \tag{5}$$

Lastly, the total malaria parasite population in the form of sporozoites, merozoites, and gametocytes at a time t is given as $N_S(t) = S(t) + M(t) + G(t)$,

$$\begin{aligned}\frac{dN_S}{dt} &= (1-\xi_3)N\delta H_I + (1-\xi_3)Q\sigma R_I - \mu_M M + \pi_S - \mu_S S \\ &\quad + cR_I - \mu_G G - \xi_4 G, \\ &\leq (1-\xi_3)N\delta H_I + (1-\xi_3)Q\sigma R_I + cR_I + \pi_S - d_3 N_S, \\ &where \ d_3 = min\{\mu_M, \mu_G, \mu_S\} \\ N_S(t) &\leq \frac{\pi_S}{d_3} \\ &\quad + \left(N_{S0} - \frac{\pi_S}{d_3} + \int_0^t (1-\xi_3)N\delta H_I + (1-\xi_3)Q\sigma R_I + cR_I dt\right) e^{-d_3 t}.\end{aligned} \tag{6}$$

Taking the limit as $t \to \infty$ for the Equations (4), (5), and (6), we obtained $N_H(t) \leq \frac{\pi_H}{d_1}$, $N_R(t) \leq \frac{\pi_R}{d_2}$, and $N_S(t) \leq \frac{\pi_S}{d_3}$. Therefore, the biologically feasible region Ω is positive invariant to the in-host malaria model (Equation 1).

3.2 Parasite-free equilibrium point

The parasite-free equilibrium point is the steady-state solution where there is no parasite in the host cell. It is obtained by setting the right-hand side of the dynamical system (1) to zero. Thus, $E_0 = (H^0, HI^0, R^0, RI^0, S^0, M^0, G^0) = (\frac{\pi_H}{\mu_H}, 0, \frac{\pi_R}{\mu_R}, 0, 0, 0, 0)$.

3.3 The basic reproduction number

The in-host basic reproduction number is the average number of secondary infections due to the introduction of sporozoites in human host cells. It is computed using the technique of the next-generation matrix approach described by Van den Driessche and Watmough [38]. We consider only the infected compartments H_I, R_I, M and G. Let F_i be the rate of new appearance and V_i be the rate of transfer from one compartment to another by any means and given as

$$F_i = \begin{pmatrix} (1-\xi_1)\beta_1 HS \\ (1-\xi_2)\beta_2 RM \\ 0 \\ 0 \\ 0 \end{pmatrix}, \tag{7}$$

$$V_i = \begin{pmatrix} \delta H_I \\ \sigma R_I \\ -\pi_S + \mu_S S \\ -(1-\xi_3)N\delta H_I - (1-\xi_3)Q\sigma R_I + \mu_M M \\ -cR_I + \xi_4 G + \mu_G G \end{pmatrix}.$$

The Jacobian matrix of vectors F and V are obtained via the differentiating F_i and V_i of the Equation (7) with respect to the infected compartments at the parasite-free equilibrium point $E_0 = (\frac{\pi_H}{\mu_H}, 0, \frac{\pi_R}{\mu_R}, 0, 0, 0, 0)$ and give as

$$F = \begin{pmatrix} 0 & 0 & (1-\xi_1)\beta_1 H_0 & 0 & 0 \\ 0 & 0 & 0 & (1-\xi_2)\beta_2 R_0 & 0 \\ 0 & 0 & 0 & 0 & 0 \\ 0 & 0 & 0 & 0 & 0 \\ 0 & 0 & 0 & 0 & 0 \end{pmatrix}, \tag{8}$$

$$V = \begin{pmatrix} \delta & 0 & 0 & 0 & 0 \\ 0 & \sigma & 0 & 0 & 0 \\ 0 & 0 & \mu_S & 0 & 0 \\ -(1-\xi_3)N\delta & -(1-\xi_3)Q\sigma & 0 & \mu_M & 0 \\ 0 & -c & 0 & 0 & \xi_4 + \mu_G \end{pmatrix}. \tag{9}$$

Hence, the inverse of the matrix V is

$$V^{-1} = \begin{pmatrix} \frac{1}{\delta} & 0 & 0 & 0 & 0 \\ 0 & \frac{1}{\sigma} & 0 & 0 & 0 \\ 0 & 0 & \frac{1}{\mu_S} & 0 & 0 \\ \frac{(1-\xi_3)N\delta}{\delta\mu_m} & \frac{(1-\xi_3)Q\sigma}{\mu_m\sigma} & 0 & \frac{1}{\mu_M} & 0 \\ 0 & \frac{c}{\sigma(\mu_g+\xi_4)} & 0 & 0 & \frac{1}{\xi_4+\mu_G} \end{pmatrix}. \tag{10}$$

The basic reproduction number $\mathcal{R}_0$ is the spectral radius of $\rho(FV^{-1})$. Thus,

$$\mathcal{R}_0 = \rho(FV^{-1}) = \frac{(1-\xi_2)(1-\xi_3)\beta_2 \pi_R Q}{\mu_R \mu_M}. \tag{11}$$

3.4 Local stability analysis of parasite-free equilibrium point

In this section, we present the local stability analysis of the parasite-free equilibrium (PFE) point, by linearizing the dynamical system (Equation 1) at E_0. The Jacobian matrix at any point is given as

$$J(E) = \begin{pmatrix} -A_1-\mu_H & 0 & 0 & 0 & -(1-\xi_1)\beta_1 H & 0 & 0 \\ A_1 & -\delta & 0 & 0 & (1-\xi_1)\beta_1 H & 0 & 0 \\ 0 & 0 & -A_2-\mu_R & 0 & 0 & -(1-\xi_2)\beta_2 R & 0 \\ 0 & 0 & A_2 & -\sigma & 0 & (1-\xi_2)\beta_2 R & 0 \\ 0 & 0 & 0 & 0 & -\mu_S & 0 & 0 \\ 0 & (1-\xi_3)N\delta & 0 & (1-\xi_3)Q\sigma & 0 & -\mu_M & 0 \\ 0 & 0 & 0 & c & 0 & 0 & -(\xi_4+\mu_G) \end{pmatrix}, \tag{12}$$

where $A_1 = (1-\xi_1)\beta_1 S$ and $A_2 = (1-\xi_2)\beta_2 M$.

Theorem 3. The parasite-free equilibrium E_0 is locally asymptotically stable if $\mathcal{R}_0 < 1$ and unstable if $\mathcal{R}_0 > 1$.

Proof 3. The Jacobian matrix at parasite-free equilibrium point E_0 is given by

$$J(E_0) = \begin{pmatrix} -\mu_H & 0 & 0 & 0 & \frac{-(1-\xi_1)\beta_1\pi_H}{\mu_H} & 0 & 0 \\ 0 & -\delta & 0 & 0 & (\frac{-(1-\xi_1)\beta_1\pi_H}{\mu_H} & 0 & 0 \\ 0 & 0 & -\mu_R & 0 & 0 & \frac{-(1-\xi_2)\beta_2\pi_R}{\mu_R} & 0 \\ 0 & 0 & 0 & -\sigma & 0 & \frac{(1-\xi_2)\beta_2\pi_R}{\mu_R} & 0 \\ 0 & 0 & 0 & 0 & -\mu_S & 0 & 0 \\ 0 & (1-\xi_3)N\delta & 0 & (1-\xi_3)Q\sigma & 0 & -\mu_M & 0 \\ 0 & 0 & 0 & c & 0 & 0 & -(\xi_4+\mu_G) \end{pmatrix}. \tag{13}$$

The eigenvalues of the Jacobian matrix, $J(E^0)$ are obtained from the corresponding characteristic polynomial equation $|J(E^0) - \lambda I| = 0$. Clearly, the first, third, and seventh column of the Jacobian matrix (Equation 13) has only diagonal entries. Thus, the eigenvalues $\lambda_1 = -\mu_H, \lambda_3 = -\mu_R$ and $\lambda_7 = -(\xi_4 + \mu_G)$. The remaining eigenvalues are obtained from the sub-matrix

$$J^1(E_0) = \begin{pmatrix} -\delta & 0 & (\frac{-(1-\xi_1)\beta_1\pi_H}{\mu_H} & 0 \\ 0 & -\sigma & 0 & \frac{(1-\xi_2)\beta_2\pi_R}{\mu_R} \\ 0 & 0 & -\mu_S & 0 \\ (1-\xi_3)N\delta & (1-\xi_3)Q\sigma & 0 & -\mu_M \end{pmatrix}. \tag{14}$$

The associated characteristic equation of the Jacobian matrix Equation (14) is $|J^1(E_0) - \lambda I| = 0$, which means

$$(\delta+\lambda)(\mu_S+\lambda)\left((\sigma+\lambda)(\mu_M+\lambda) - \frac{(1-\xi_3)(1-\xi_2)\beta_2\pi_R\sigma Q}{\mu_R}\right) = 0. \tag{15}$$

Simply, we have $\lambda_2 = -\delta, \lambda_5 = -\mu_S$, and the remaining eigenvalues are obtained from the equation

$$\lambda^2 + B_1\lambda + B_0 = 0, \tag{16}$$

where

$$B_0 = \sigma + \mu_M, \text{ and } B_1 = \mu_M\sigma - \frac{(1-\xi_3)(1-\xi_2)\beta_2\pi_R\sigma Q}{\mu_R}.$$

Applying Routh–Hurwitz stability criterion, the characteristic Equation (16) has roots with a negative real part if $B_0 > 0$ and $B_1 > 0$. Obviously, $B_0 > 0$. We now need to show $B_1 > 0$. Now,

$$\begin{aligned} B_1 &= \mu_M\sigma - \frac{(1-\xi_3)(1-\xi_2)\beta_2\pi_R\sigma Q}{\mu_R}, \\ &= \mu_M\sigma\left(1 - \frac{(1-\xi_3)(1-\xi_2)\beta_2\pi_R Q}{\mu_R\mu_M}\right), \\ &= \mu_M\sigma\,(1-\mathcal{R}_0)\,. \end{aligned}$$

We observe that $B_1 > 0$ if $\mathcal{R}_0 < 1$. Therefore, the parasite-free equilibrium point is locally asymptotically if $\mathcal{R}_0 < 1$ and unstable if $\mathcal{R}_0 > 1$.

3.5 Global stability analysis of parasite-free equilibrium point

Here, we provide the global stability analysis of a parasite-free equilibrium point using a suitable Lypounove function.

Theorem 4. If $\mathcal{R}_0 \leq 1$, then the parasite-free equilibrium E_0 is globally asymptotically stable.

Proof 4. A suitable Lyapunov functional defined as

$$\begin{aligned} L = N(H - H^0 - H^0\ln\frac{H}{H^0}) + NH_I + Q(R - R^0 - \ln\frac{R}{R^0}) \\ + NR_I + QR_I + S + \frac{1}{1-\xi_3}M + QG. \end{aligned}$$

A Lyapunov functional L is non-negative and strictly minimized to the parasite-free equilibrium point. We now compute the derivative of L as follows:

$$\begin{aligned} \frac{dL}{dt} =& N\left(1 - \frac{H^0}{H}\right)\frac{dH}{dt} + N\frac{dH_I}{dt} + Q\left(1 - \frac{R^0}{R}\right)\frac{dR}{dt} + Q\frac{dR_I}{dt} \\ &+ \frac{dS}{dt} + \frac{1}{1-\xi_3}\frac{dM}{dt} + Q\frac{dG}{dt} \end{aligned}$$

$$
\begin{aligned}
=&N\left(1-\frac{H^0}{H}\right)(\pi_H-(1-\xi_1)\beta_1 HS-\mu_H H)\\
&+N((1-\xi_1)\beta_1 HS-\delta H_I)\\
&+Q\left(1-\frac{R^0}{R}\right)(\pi_R-(1-\xi_2)\beta_2 RM-\mu_R R)\\
&+Q((1-\xi_2)\beta_2 RM-\sigma R_I)\\
&+\pi_S-\mu_H S+\frac{1}{1-\xi_3}((1-\xi_3)N\delta H_I\\
&+(1-\xi_3)Q\sigma R_I-\mu_M M)+cR_I-\xi_4 G-\mu_G G\\
=&N\left(1-\frac{H^0}{H}\right)(\mu_H H^0-(1-\xi_1)\beta_1 HS-\mu_H H)\\
&+N((1-\xi_1)\beta_1 HS-\delta H_I)\\
&+Q\left(1-\frac{R^0}{R}\right)(\mu_R R^0-(1-\xi_2)\beta_2 RM-\mu_R R)\\
&+Q((1-\xi_2)\beta_2 RM-\sigma R_I)+\mu_S S^0-\mu_S S\\
&\frac{1}{1-\xi_3}((1-\xi_3)N\delta H_I+(1-\xi_3)Q\sigma R_I-\mu_M M)+cR_I\\
&-\xi_4 G-\mu_G G\\
&=-\mu_H N\frac{(H-H^0)^2}{H}-N(1-\xi_1)\beta_1 HS+N(1-\xi_1)\beta_1 HS\\
&+\frac{H^0}{H}(1-\xi_1)\beta_1 HS\\
&-\mu_R Q\frac{(R-R^0)^2}{R}-Q(1-\xi_2)\beta_2 MR+Q(1-\xi_2)\beta_2 MR\\
&+\frac{R^0}{R}Q(1-\xi_2)\beta_2 MR-\frac{\mu_M M}{1-\xi_3}\\
&+\mu_S S^0-\mu_S S-QcR_I+QcR_I-(\xi_4+\mu_G)G\\
&=-\mu_H N\frac{(H-H^0)^2}{H}+\frac{\pi_H}{\mu_H}(1-\xi_1)\beta_1 S-\mu_R Q\frac{(R-R^0)^2}{R}\\
&+\frac{\pi_R}{\mu_R}Q(1-\xi_2)\beta_2 M-\mu_S S-\frac{\mu_M M}{1-\xi_3}-(\xi_4+\mu_G)G\\
&=-\mu_H N\frac{(H-H^0)^2}{H}-\mu_R Q\frac{(R-R^0)^2}{R}\\
&+\frac{\mu_M}{(1-\xi_3)}(\mathcal{R}0-1)M-\mu_S\left(1-\frac{S^0}{S}-\frac{\pi_H(1-\xi_1)\beta_1}{\mu_H\mu_S}\right)S\\
&-(\xi_4+\mu_G)G.
\end{aligned}
$$

The expression $\frac{dL}{dt}\leq 0$ if $R_0<1$ and $\frac{S^0}{S}+\frac{\pi_H(1+\xi_1)\beta_1}{\mu_H\mu_S}\leq 1$ for any positive H, H_I, R, R_I, S, M, G. The equality $\frac{dL}{dt}=0$, holds if and only if for $H=H^0$, $R=R^0, G=G^0$, $\mathcal{R}_0=1$, and $\pi_H(1-\xi_1)\beta_1/\mu_H\mu_S+S^0/S=1$. Therefore, by LaSalle's Invariance Principle [39], the parasite-free equilibrium E_0 is global asymptotically stable for $\mathcal{R}_0<1$.

3.6 Parasite persistence equilibrium point

The parasite persistence equilibrium point is the steady-state solution at which the malaria parasite persists in the host cells. It is computed by setting the right hand side of the system Equation (1) to zero. The parasite persistence equilibrium point E^* is investigated and given as

$$
E^*(H^*,H_I^*,R^*,R_I^*,S^*,M^*,G^*)=\begin{cases}
H^*=\frac{\pi_H}{(1-\xi_1)\beta_1\frac{\pi_S}{\mu_S}+\mu_H},\\
H_I^*=\frac{(1-\xi_1)\beta_1\pi_S\pi_H}{\delta(\mu_S(1-\xi_1)\frac{\pi_S}{\mu_S}+\mu_H)},\\
R^*=\frac{\pi_R}{(1-\xi_2)\beta_2 M^*+\mu_R},\\
R_I^*=\frac{(1-\xi_2)\pi_R\beta_2 M^*}{((1-\xi_2)\beta_2 M^*+\mu_R)\sigma}\\
S^*=\frac{\pi_S}{\mu_S},\\
G^*=\frac{c(1-\xi_2)\pi_R\beta_2 M^*}{((1-\xi_2)\beta_2 M^*+\mu_R)\sigma(\xi_4+\mu_G)},
\end{cases}
$$

where M^* is the positive roots of

$$
P(M^*)=d_0M^{*2}+d_1M^*+d_2=0, \tag{17}
$$

and the coefficients d_2, d_1, and d_0 are given as

$$
\begin{aligned}
d_0=&\ \mu_S(1-\xi_1)\frac{\pi_S}{\mu_S}+\mu_H\mu_M(1-\xi_2)\beta_2\sigma,\\
d_1=&\ (\mu_S(1-\xi_1)\frac{\pi_S}{\mu_S}+\mu_H)\mu_M\mu_R\sigma\,(1-\mathcal{R}_0)\\
&-(1-\xi_3)N(1-\xi_1)\beta_1\pi_S\pi_H(1-\xi_2)\beta_2\sigma,\\
d_2=&-(1-\xi_3)N(1-\xi_1)\beta_1\pi_S\pi_H\mu_R(\sigma+c).
\end{aligned} \tag{18}
$$

By Descarts' rule of sign, the system Equation (1) has a parasite persistence equilibrium, if $d_1<0$ implies that $R_0>1$ and/or if $d_1<0$ implies that $R_0>1$, and if the discriminant $\Delta=0$, where

$$
\begin{aligned}
\Delta=&d_1^2-4d_2d_0\\
=&\Big((\mu_S(1-\xi_1)\frac{\pi_S}{\mu_S}+\mu_H)\mu_M\mu_R(\sigma+c)\,(1-\mathcal{R}_0)\\
&-(1-\xi_3)N(1-\xi_1)\beta_1\pi_S\pi_H(1-\xi_2)\beta_2\sigma\Big)^2,\\
&+4(\mu_S(1-\xi_1)\frac{\pi_S}{\mu_S}+\mu_H)(\mu_M(1-\xi_2)\beta_2\sigma)(1-\xi_3)N(1\\
&-\xi_1)\beta_1\pi_S\pi_H\mu_R(\sigma+c).
\end{aligned}
$$

From Equation (18), it is not difficult to see that d_0 is always positive and d_2 is negative. Thus, by Descarts' rule of sign and/or discriminant, a parasite persistence equilibrium point exists if $R_0>1$.

3.7 Local stability analysis of parasite persistence equilibrium point

In this section, we examine the local stability analysis of parasite persistence equilibrium via linearzing the system Equation (1) at E^*.

Theorem 5. The parasite persistence equilibrium point is locally asymptotically stable if $R_0>1$ and unstable if $R_0<1$.

Proof 5. The Jacobian matrix at parasite persistence equilibrium, E^* is given as

$$J(E^*) = \begin{pmatrix} -A_1-\mu_H & 0 & 0 & 0 & -(1-\xi_1)\beta_1 H & 0 & 0 \\ A_1 & -\delta & 0 & 0 & (1-\xi_1)\beta_1 H & 0 & 0 \\ 0 & 0 & -A_2-\mu_R & 0 & 0 & -(1-\xi_2)\beta_2 R^* & 0 \\ 0 & 0 & A_2 & -\sigma & 0 & (1-\xi_2)\beta_2 R^* & 0 \\ 0 & 0 & 0 & 0 & -\mu_S & 0 & 0 \\ 0 & (1-\xi_3)N\delta & 0 & (1-\xi_3)Q\sigma & 0 & -\mu_M & 0 \\ 0 & 0 & 0 & c & 0 & 0 & -(\xi_4+\mu_G) \end{pmatrix}, \tag{19}$$

where $A_1 = (1-\xi_1)\beta_1 S^*$ and $A_2 = (1-\xi_2)\beta_2 M^*$.

The associated characteristic equation is given as $det(J(E^*) - \lambda I) = 0$. To simplify the steps now, the last column of the Jacobian matrix (19) has only diagonal entry; thus, we have $\lambda_7 = -(\xi_4+\mu_G)$. The fifth row of the Jacobian matrix has only a diagonal entry, and we can easily obtain the $\lambda_5 = -\mu_S$. The remaining eigenvalues are obtained from the submatrix

$$J_1(E^*) = \begin{pmatrix} -A_1-\mu_H & 0 & 0 & 0 & 0 \\ A_1 & -\delta & 0 & 0 & 0 \\ 0 & 0 & -A_2-\mu_R & 0 & -(1-\xi_2)\beta_2 R^* \\ 0 & 0 & A_2 & -\delta & (1-\xi_2)\beta_2 R^* \\ 0 & (1-\xi_3)N\delta & 0 & (1-\xi_3)Q\sigma & -\mu_M \end{pmatrix}. \tag{20}$$

The associated characteristic equation is given as $det(J_1(E^*) - \lambda I) = 0$. Thus,

$$(A_1+\mu_H+\lambda)(\delta+\lambda)(\lambda^3 + B_0\lambda^2 + B_1\lambda + B_0) = 0, \tag{21}$$

where

$$B_0 = \delta + \mu_M + A_2 + \mu_R,$$
$$B_1 = \delta\mu_M + (A_2+\mu_R)(\delta+\mu_M),$$
$$B_2 = \delta\mu_M(A_2+\mu_R) - (1-\xi_2)(1-\xi_3)Q\delta\beta_2 R^* + (1-\xi_2)(1-\xi_3)\beta_2 A_2 Q\delta R^*.$$

From characteristic polynomial Equation (21), we have $\lambda_1 = -A_1 - \mu_H, \lambda_2 = -\delta$ or

$$\lambda^3 + B_0\lambda^2 + B_1\lambda + B_0 = 0. \tag{22}$$

Applying the Routh-Hurwitz stability criteria, the polynomial Equation (22) has roots with negative real part if $B_0 > 0, B_1 > 0$, $B_2 > 0$, and $B_2 - B_0B_1 > 0$. Therefore, the parasite persistence equilibrium point is locally asymptotically stable if $R_0 > 1$. This completes the proof.

3.8 Sensitivity analysis

In this section, we present the sensitivity analysis for the basic reproduction number $\mathcal{R}_0$ to identify the parameters that have a high impact on disease elaboration within the host. The normalized forward sensitivity index of a variable to a parameter is the ratio of the relative change in the variable to the relative change in the parameter. If the variable is a differentiable function

TABLE 3 Sensitivity index of within-host basic reproduction number $\mathcal{R}_0$.

Parameters	Elasticity index	Value	Parameters	Elasticity index	Value
β_2	$\Theta^{\mathfrak{R}_0}_{\beta_2}$	+1	π_R	$\Theta^{\mathfrak{R}_0}_{\pi_R}$	+1
Q	$\Theta^{\mathfrak{R}_0}_{Q}$	+1	μ_M	$\Theta^{\mathfrak{R}_0}_{\mu_M}$	−1
μ_R	$\Theta^{\mathfrak{R}_0}_{\mu_R}$	−1			

TABLE 4 Model parameter values.

Parameters	Value	Units	Source	Parameters	Value	Units	Source
π_S	30	sporozoite /day	[40]	μ_S	1.2×10^{-11}	/day	[41]
π_H	3000	cells/ml/day	[41]	μ_R	0.0083	/day	[42]
π_R	3×10^5	cells/day/μl	[40]	σ	1.0	/day	[24]
β_1	$0.001\mu l$	μl/cell/day	[43]	μ_G	0.0000625	/day	[41]
β_2	2×10^{-6}	/sporozoite	Estimated	c	0.02	/day	[44]
δ	0.02	cell/day	[40]	μ_H	0.029	cell/day	[40]
N	10000	/day	[41]	Q	16	/day	[45]
μ_M	48	/day	[45]				

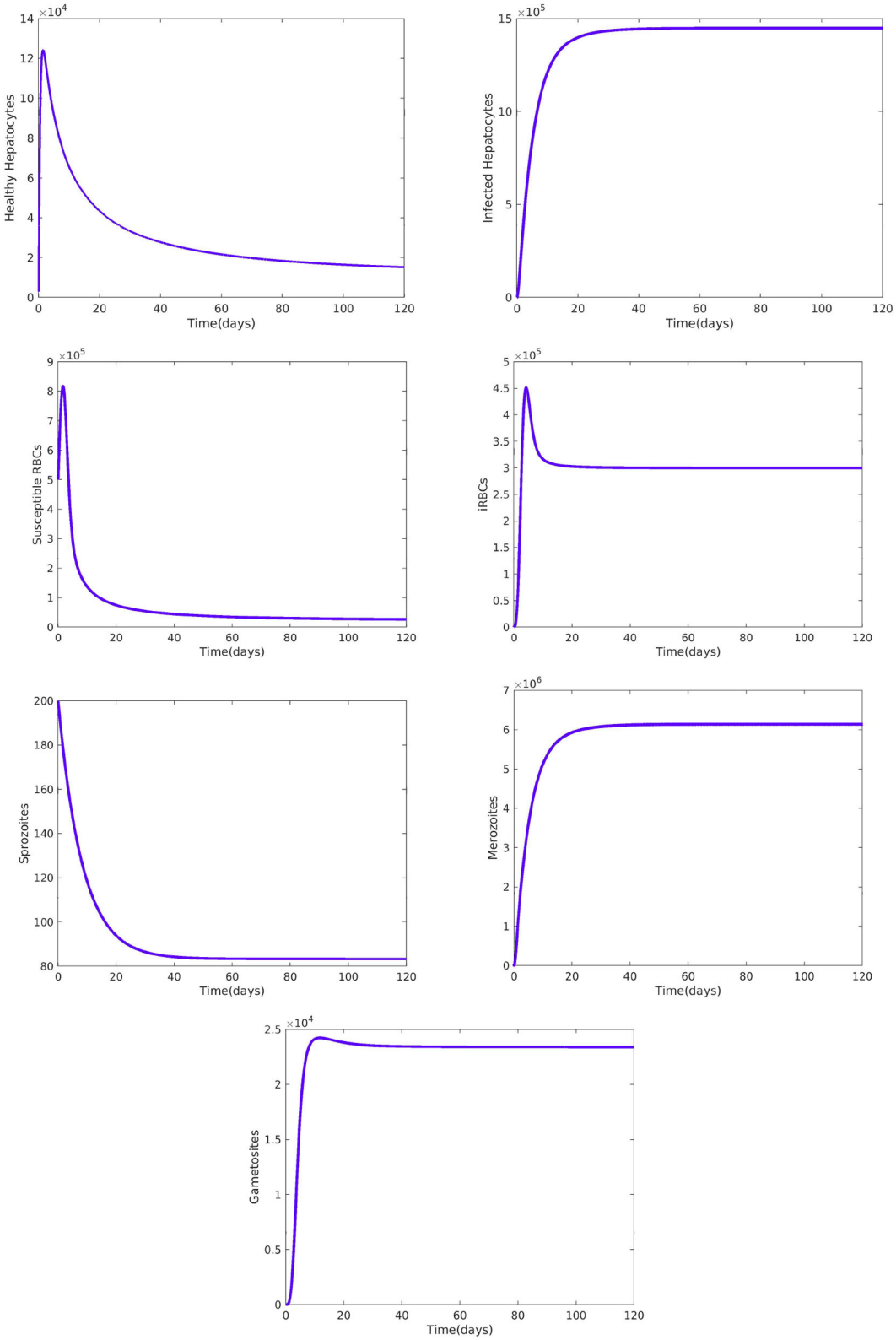

FIGURE 2
Dynamical behavior of the system Equation (1) without malaria drug treatments, i.e., $\xi_1 = 0, \xi_2 = 0, \xi_3 = 0, \xi_4 = 0, \mathcal{R}_0 = 24.695$ and all the other parameters are fixed as in Table 4.

of the parameter, the sensitivity index is then defined using partial derivatives .

Definition: The normalized forward sensitivity index of a variable M that depends differentiability on a parameter u is defined as

$$\Theta_u^M = \frac{\partial M}{\partial u} \times \frac{u}{M}$$

As we have an explicit formula for R_0 given in Equation (11), we derive an analytical expression for the sensitivity of R_0

$$\Theta_\vartheta^{\mathcal{R}_0} = \frac{\partial \mathcal{R}_0}{\partial \vartheta} \times \frac{\vartheta}{\mathcal{R}_0},$$

where ϑ is represented the model parameters which belongs to basic reproduction number $\mathcal{R}_0$. Now,

$$\Theta_{\beta_2}^{\mathcal{R}_0} = \frac{\partial \mathcal{R}_0}{\partial \beta_2} \times \frac{\beta_2}{\mathcal{R}_0} = +1, \qquad \Theta_{\pi_R}^{\mathcal{R}_0} = \frac{\partial \mathcal{R}_0}{\partial \pi_R} \times \frac{\pi_R}{\mathcal{R}_0} = +1,$$
$$\Theta_Q^{\mathcal{R}_0} = \frac{\partial \mathcal{R}_0}{\partial Q} \times \frac{Q}{\mathcal{R}_0} = +1, \qquad \Theta_{\mu_M}^{\mathcal{R}_0} = \frac{\partial \mathcal{R}_0}{\partial \mu_M} \times \frac{\mu_M}{\mathcal{R}_0} = -1$$
$$\Theta_{\mu_R}^{\mathcal{R}_0} = \frac{\partial \mathcal{R}_0}{\partial \mu_R} \times \frac{\mu_R}{\mathcal{R}_0} = -1.$$

From Table 3, we see that the infection rate of the erythrocyte by merozoites β_2, average number of merozoites per ruptured infected erythrocyte cells Q, the production rate of the uninfected

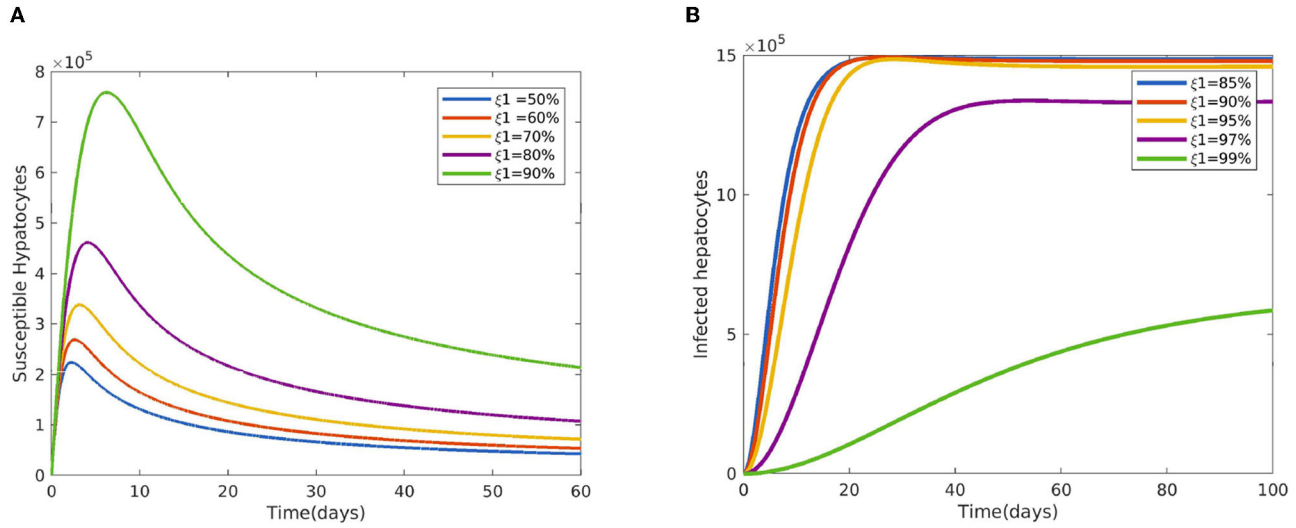

FIGURE 3
Impact of primary tissue schizontocides (pre-erythrocytic treatment) ξ_1 **(A)** on susceptible hepatocytes **(B)** on infected hepatocytes using the following parameter values: $\pi_S = 30, \pi_H = 3000, \pi_R = 3 \times 10^5, \beta_1 = 0.001, \beta_2 = 2 \times 10^{-6}, \delta = 0.02, N = 10000, \mu_M = 48, \mu_S = 1.2 \times 10^{-11}, \mu_R = 0.0083, \sigma = 1.0, \mu_G = 0.0000625, c = 0.02, \mu_H = 0.029, Q = 16$ and all the other parameters are fixed as in Table 4.

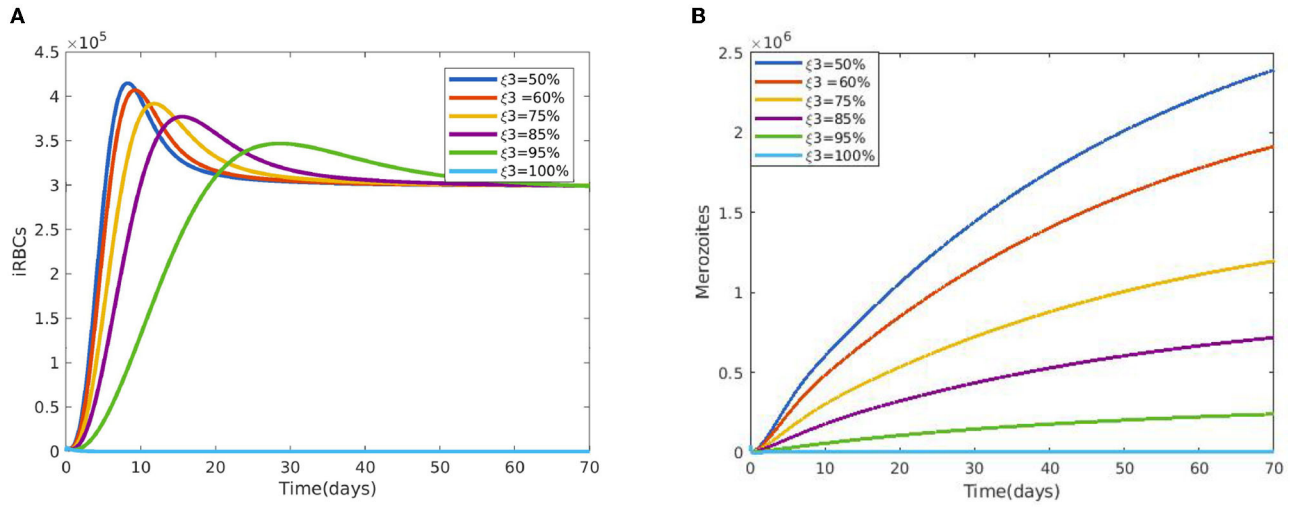

FIGURE 4
(A) Impact of blood schizontocides ξ_3 on iRBCs. **(B)** Impact of blood schizontocides ξ_3 on merozoites using the following parameter values: $\pi_S = 30, \pi_H = 3,000, \pi_R = 3 \times 10^5, \beta_1 = 0.001, \beta_2 = 2 \times 10^{-6}, \delta = 0.02, N = 10,000, \mu_M = 48, \mu_S = 1.2 \times 10^{-11}, \mu_R = 0.0083, \sigma = 1.0, \mu_G = 0.0000625, c = 0.02, \mu_H = 0.029, Q = 16$ and all the other parameters are fixed as in Table 4.

erythrocyte π_R, natural death rate merozoites μ_M, and natural death rate of red-blood cells μ_R are the most sensitive parameters. A 10% increase (or decrease) in β_2, Q, and π_R is a 10% increase (or decrease) in $\Re_0$. A 10% increase (decrease) in μ_M and μ_R is a 10% decrease (or increase) in $\Re_0$.

4 Numerical simulations

In this section, we present the numerical simulation of model (Equation 1) in order to supplement the analytical results. The initial condition we used in this simulation is $H(0) = 3000, H_I(0) = 10, R(0) = 500000, R_I(0) = 200, S(0) = 200, M(0) = 40,000$, and $G(0) = 20$, and the model parameters are given in Table 4. Using the model parameter values, we have within host basic reproduction number $\mathcal{R}_0 = 24.0964$ without antimalarial drug treatment ($\xi_1 = 0, \xi_2 = 0$) and $\mathcal{R}_0 = 6.0241$ with antimalarial drug treatment 50% effective ($\xi_1 = 50\%, \xi_2 = 50\%$ effective). The simulation of the system equations are integrated using the ode45 solver in MATLAB.

Figure 2 reveals the dynamical behavior of model (Equation 1) in the absence of antimalarial drug treatments, i.e., all-stage

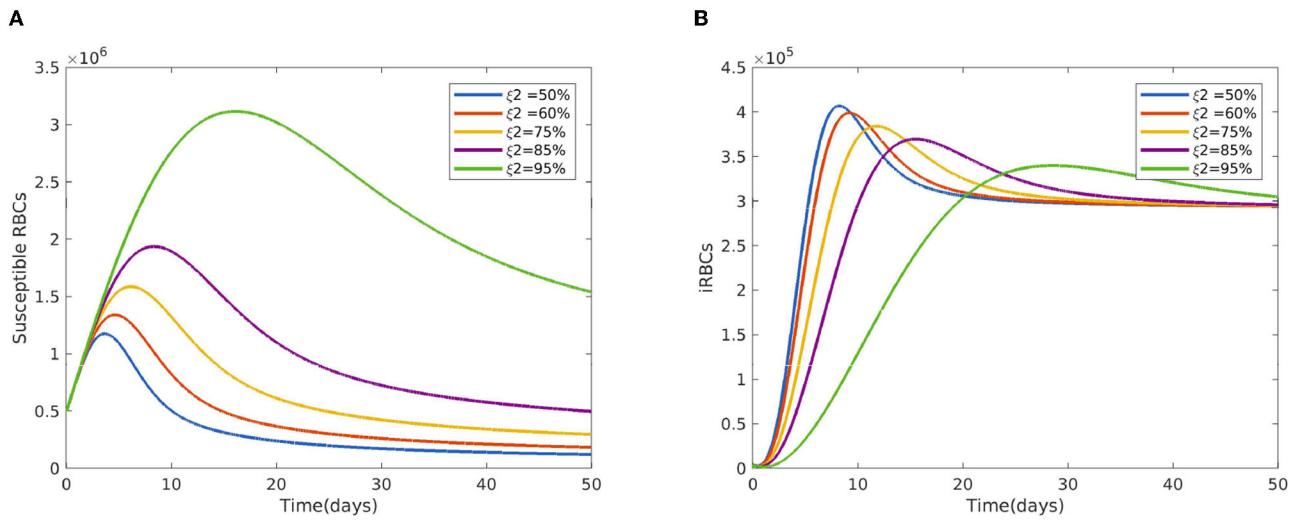

FIGURE 5
Impact of the blood schizontocides ξ_2 **(A)** on healthy RBCs **(B)** on iRBCs using the following parameter values: $\pi_S = 30, \pi_H = 3000, \pi_R = 3 \times 10^5, \beta_1 = 0.001, \beta_2 = 2 \times 10^{-6}, \delta = 0.02, N = 10,000, \mu_M = 48, \mu_S = 1.2 \times 10^{-11}, \mu_R = 0.0083, \sigma = 1.0, \mu_G = 0.0000625, c = 0.02, \mu_H = 0.029, Q = 16$ and all the other parameters are fixed as in Table 4.

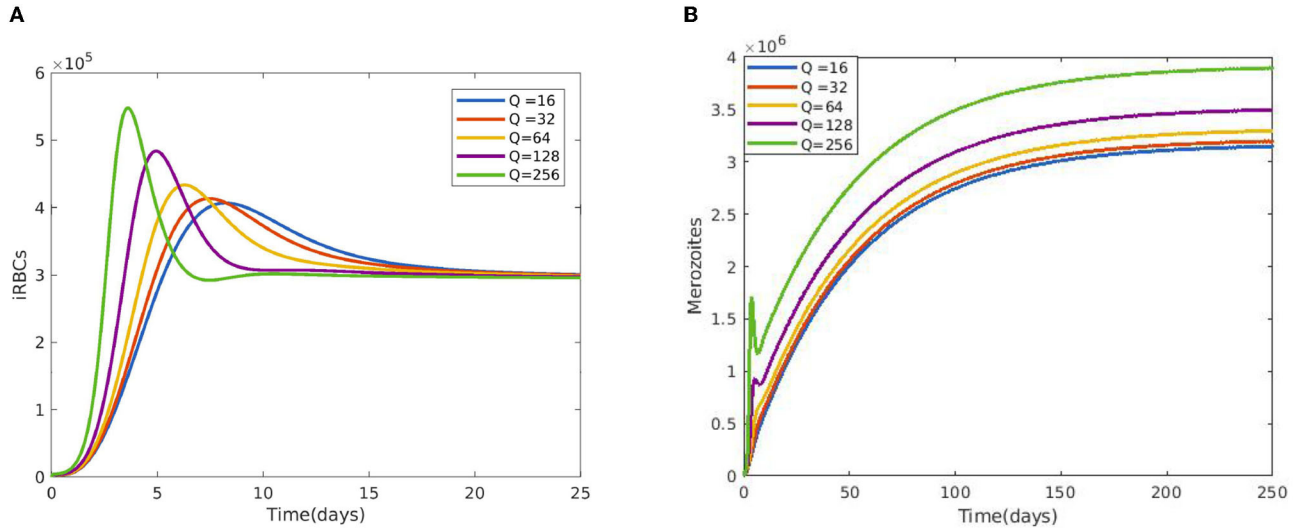

FIGURE 6
Impact of average number of merozoites per ruptured infected erythrocyte cells Q **(A)** on iRBCs and **(B)** on merozoites using the following parameter values: $\pi_S = 30, \pi_H = 3,000, \pi_R = 3 \times 10^5, \beta_1 = 0.001, \beta_2 = 2 \times 10^{-6}, \delta = 0.02, N = 10,000, \mu_M = 48, \mu_S = 1.2 \times 10^{-11}, \mu_R = 0.0083, \sigma = 1.0, \mu_G = 0.0000625, c = 0.02, \mu_H = 0.029, Q = 16$ and all the other parameters are fixed as in Table 4.

antimalarial drug treatment is not administered ($\xi_1 = 0, \xi_2 = 0, \xi_3 = 0$, and $\xi_4 = 0$). The vulnerable hepatocytes and red blood cells decrease over time, whereas the other state variables are rise. All the system solutions converge to an endemic equilibrium point. The effect of primary tissue schizontocides on healthy and infected hepatocytes is shown in Figure 3. As metformin's antimalarial effectiveness rises, the number of healthy hepatocytes also rises (see Figure 3A). Figure 3B reveals that when the effectiveness of metformin antimalarial treatment rises, the number of infected hepatocytes declines. Figure 4A shows the iRBCs decrease as the efficiency of blood schizontocides increases. Figure 4B indicates the impact of blood schizontocide and primary tissue schizontocide on merozoites. The merozoite population decreases as the blood schizontocides and primary tissue schizontocides efficiency increases. The impact of blood schizontocides (blood-stage antimalarial medication treatment) on red blood cells is depicted in Figure 5. As blood schizontocides (blood-stage antimalarial drug therapy) increases, the number of uninfected red blood cells rises (see Figure 5A). As indicated in Figure 5B, the infected red blood cells gradually declines as the

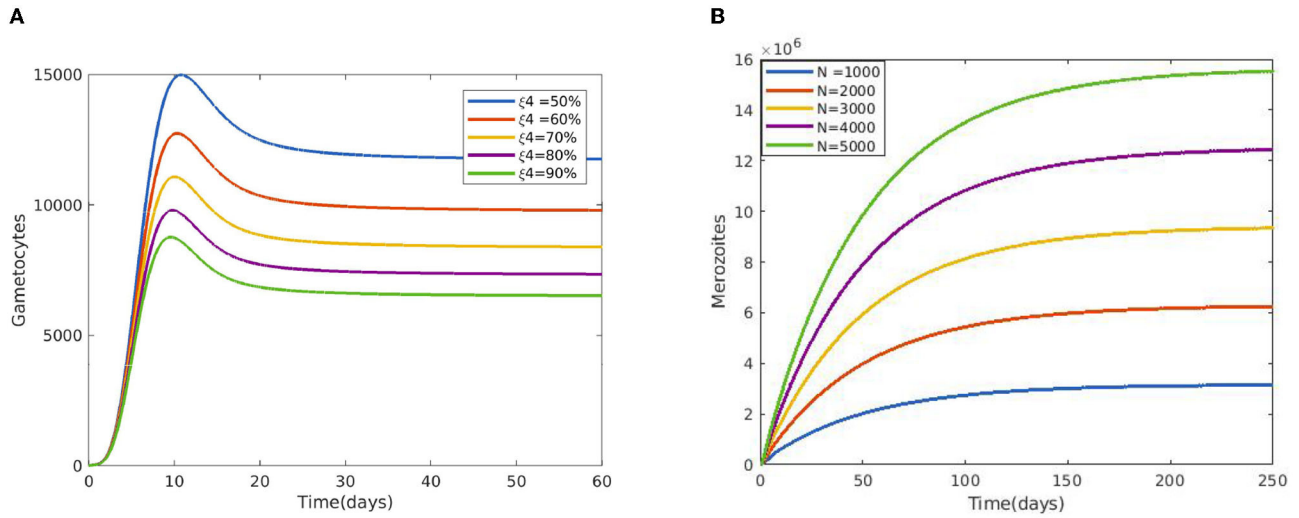

FIGURE 7
(A) Impact of gametocytocidal drugs (gametocytocides) on sexual replication of malaria parasites. **(B)** Effect of the average number of merozoite released per ruptured infected hepatocytic cells using the following parameter values: $\pi_S = 30, \pi_H = 3,000, \pi_R = 3 \times 10^5, \beta_1 = 0.001, \beta_2 = 2 \times 10^{-6}, \delta = 0.02, \mu_M = 48, \mu_S = 1.2 \times 10^{-11}, \mu_R = 0.0083, \sigma = 1.0, \mu_G = 0.0000625, c = 0.02, \mu_H = 0.029, Q = 16$ and all the other parameters are fixed as in Table 4.

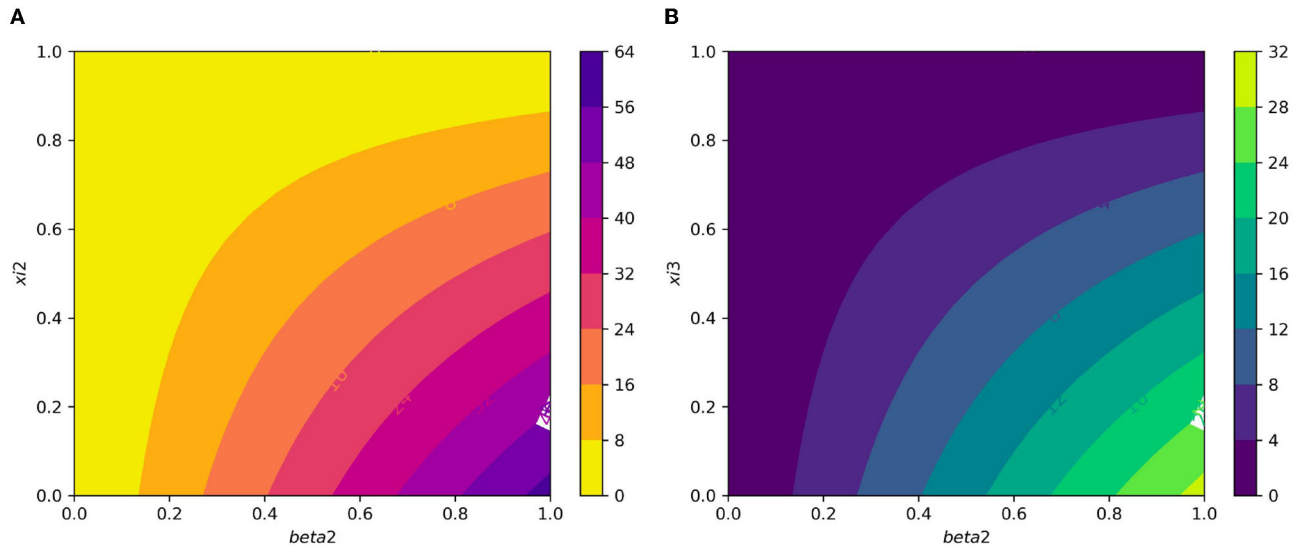

FIGURE 8
(A) Contour plot of $\mathcal{R}_0$ with respect to infection rate of the erythrocyte β_2 and efficacy of antimalarial treatment on erythrocytic invasion (blood schizontocides efficacy) ξ_2. **(B)** Contour plot of $\mathcal{R}_0$ with respect to the infection rate of the erythrocyte β_2 and efficiency of antimalarial drug treatments on the bursting rate of erythrocytic (blood schizontocides efficacy) ξ_3.

blood schizontocides (antimalarial drug treatment at the blood-stage) increases. Figure 6 demonstrates that as the average number of merozoites per ruptured infected erythrocyte grows, both the population of merozoites and the infected RBCs increases.

Figure 7A displays the gametocyte population declines as the effectiveness of gametocytocidal medication therapy (gametocytocidal) increases. Figure 7B exhibits the effect of the average number of merozoites discharged per ruptured infected hepatocytic cell on merozoites. As the average number of merozoites discharged per ruptured infected hepatocytic cell increases, the merozoite population increases. Figure 8A depicts the impact of the infection rate of erythrocyte β_2 and the antimalarial treatment on erythrocytic invasion (blood schizontocides efficacy) ξ_2 on the basic reproduction number R_0. Figure 8B displays the impact of the infection rate of the erythrocyte β_2 and blood schizontocides drug treatment ξ_3 on the basic reproduction number R_0. As imagined, to reduce the R_0 value below unity, the infection rate of the erythrocyte must be very low, almost irrespective of the blood schizontocides. That is, despite the availability of antimalarial treatment, inconsiderate mixing needs to be observed to prevent an excessive number of parasites inside the host cell. Figure 9A indicates the influence of

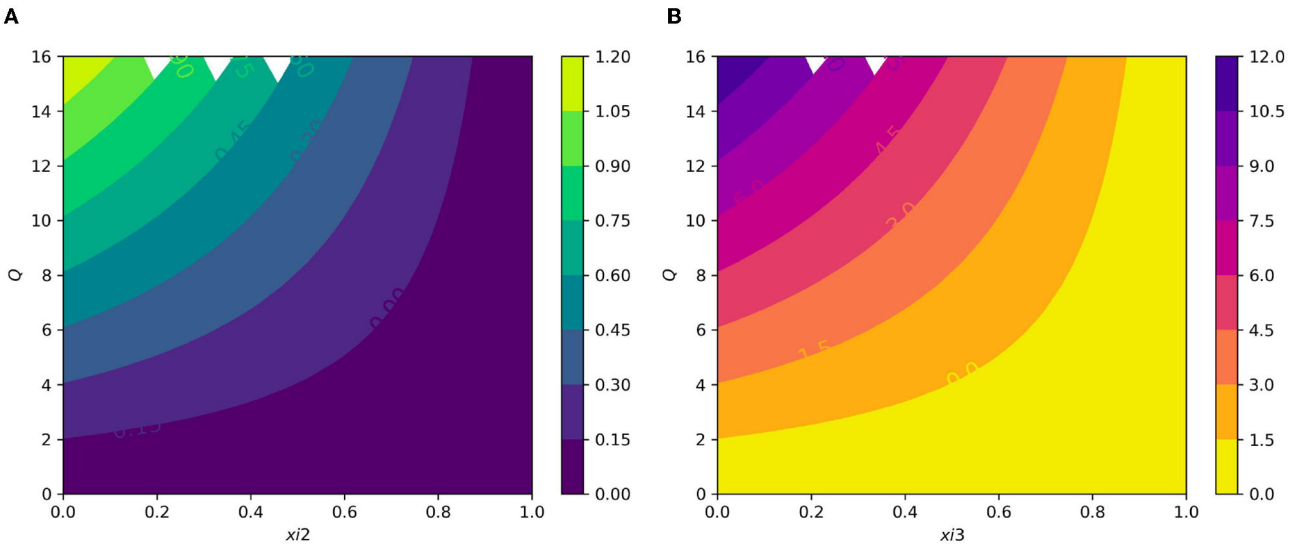

FIGURE 9
(A) Contour plot of $\mathcal{R}_0$ with respect to the average number of merozoite per ruptured infected erythrocyte cells Q and blood stage antimalarial drug treatment (efficacy of antimalarial treatment on erythrocytic invasion) ξ_2. **(B)** Contour plot of $\mathcal{R}_0$ average number of merozoite per ruptured infected erythrocyte cells Q and efficiency of antimalarial drug treatments on the bursting rate of pre-erythrocytic schizont and blood schizont ξ_3.

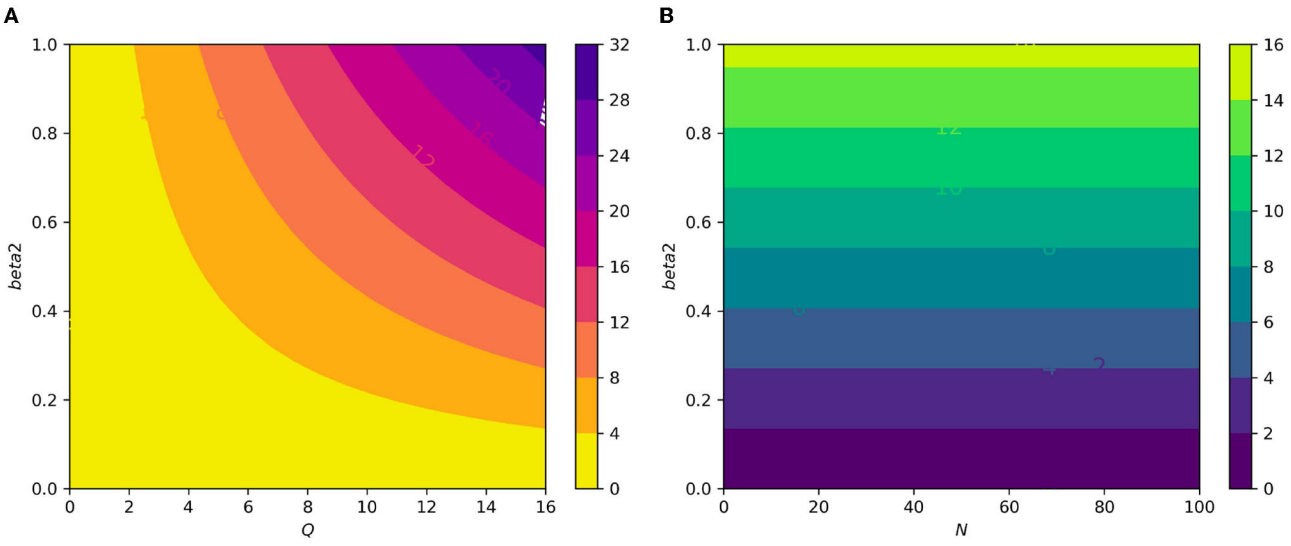

FIGURE 10
(A) Contour plot of $\mathcal{R}_0$ with respect to the infection rate of the erythrocyte β_2 and an average number of merozoite per ruptured infected erythrocyte cells Q. **(B)** Contour plot of $\mathcal{R}_0$ with respect to an infection rate of the erythrocyte β_2 and an average number of merozoite per ruptured infected hepatocyte cells N.

the average number of merozoite per ruptured infected erythrocyte cell Q and blood-stage antimalarial drug treatment (efficacy of antimalarial treatment on erythrocytic invasion) ξ_2 on the basic reproduction number R_0. Figure 9B shows the impact of the average number of merozoite per ruptured infected erythrocyte cells Q and efficiency of antimalarial drug treatments on the bursting rate of pre-erythrocytic schizont and blood schizont ξ_3. The figures illustrates decreasing the average number of merozoites per ruptured infected erythrocyte cell Q and raising blood-stage antimalarial drug treatment ξ_2 and blood schizontocide ξ_3 decreases the in-host basic reproduction number R_0, which, in turn, decreases the in-host malaria parasite. Figure 10A exhibits the impact of the infection rate of erythrocyte β_2 and the average number of merozoite per ruptured infected erythrocyte cells Q on the basic reproduction number, R_0. The within-host basic reproduction number is rises as both the infection rate of the erythrocyte and the average number of merozoite per ruptured infected erythrocyte cells increases. Figure 10B demonstrates the within-host reproduction number increases as the infection rate of the erythrocyte increases; however, the average number of merozoites per ruptured infected hepatocyte cell N has no impact on the reproduction number.

5 Conclusion

In this study, we investigated a cell-level mathematical model for malaria parasite infection with antimalarial drug treatment. The model includes the interactions of hepatocyte cells, red blood cells, and malaria parasites. The qualitative analysis of the developed model, such as the positivity, and boundedness of the solution is discussed. The equilibria and their stability analysis are investigated, where the parasite-free equilibrium point is both local and global stable if the basic reproduction number $\mathcal{R}_0$ is less than unity. The global stability analysis of the parasite-free equilibrium point is investigated using a suitable Lyponove function. The existence of parasite persistence equilibrium points is reached using Descarts' rule of sign and its local stability is investigated by applying Routh-Hurwitz stability criterion. We computed a sensitivity analysis of the in-host basic reproduction number to investigate most influential parameters in the within-host malaria parasites using the normalized forward sensitivity index. As a result, the infection rate of the erythrocyte by merozoites, the average number of merozoites per ruptured infected erythrocyte, the natural death rate of merozoites, and the requirement rate of the uninfected erythrocytes are the most influential ones. Different numerical simulations are performed to supplement our analytical findings and it is observed to be in good agreement. Furthermore, the simulation result reveals that the administration of antimalarial drug treatment, such as primary tissue schizontocides, blood schizontocides, and gametocytocides, are used to the eliminate the malaria parasites from the human host cells. This study's findings offer guidance for antimalarial medication therapy and malaria control. By lowering the average number of merozoites per ruptured infected infected erythrocyte and hepatocyte, we can restrict the generation of malaria parasites within the host and prevent them from being infected. Primary tissue schizontocide and blood-stage schizontocides will be administered in order to achieve this. In this study, we consider the constant antimalarial treatment and single strains of malaria infection. In future, we will extend it to optimal control problems using time-dependent antimalarial drug treatment, fractional order differential equations in order to investigate the memory effect, and different strains of malaria infection.

Data availability statement

The original contributions presented in the study are included in the article/supplementary material, further inquiries can be directed to the corresponding author.

Ethics statement

Ethical review and approval was not required for the study on human participants in accordance with the local legislation and institutional requirements. Written informed consent from the patients/participants was not required to participate in this study in accordance with the national legislation and the institutional requirements.

Author contributions

JA: Conceptualization, Formal analysis, Investigation, Methodology, Software, Writing – original draft, Writing – review & editing. GT: Supervision, Visualization, Writing – original draft, Writing – review & editing. SD: Investigation, Supervision, Visualization, Writing – review & editing.

Funding

The author(s) declare that no financial support was received for the research, authorship, and/or publication of this article.

Acknowledgments

The authors acknowledge Adama Science and Technology University for its support during this research work.

Conflict of interest

The authors declare that the research was conducted in the absence of any commercial or financial relationships that could be construed as a potential conflict of interest.

Publisher's note

All claims expressed in this article are solely those of the authors and do not necessarily represent those of their affiliated organizations, or those of the publisher,

the editors and the reviewers. Any product that may be evaluated in this article, or claim that may be made by its manufacturer, is not guaranteed or endorsed by the publisher.

References

1. Jagannathan P, Kakuru A. Malaria in 2022: increasing challenges, cautious optimism. *Nat Commun*. (2022) 13:2678. doi: 10.1038/s41467-022-30133-w

2. WHO. *World malaria report 2022*. Geneva: World Health Organization (2022).

3. Rosenthal PJ. Malaria in 2022: challenges and progress. *Am J Trop Med Hyg*. (2022) 106:1565. doi: 10.4269/ajtmh.22-0128

4. Agnandji ST, Fernandes JF, Bache EB, Ramharter MP. Clinical development of RTS, S/AS malaria vaccine: a systematic review of clinical Phase I-III trials. *Future Microbiol*. (2015) 10:1553–78. doi: 10.2217/fmb.15.90

5. Dhangadamajhi G, Kar SK, Ranjit MR. The survival strategies of malaria parasite in the red blood cell and host cell polymorphisms. *Malaria Res Treat*. (2010) 2010:973094. doi: 10.4061/2010/973094

6. Risco-Castillo V, Topçu SH, Carine MP, Manzoni G, Bigorgne AE, Briquet S, et al. Malaria sporozoites traverse host cells within transient vacuoles. *Cell Host Microbe*. (2015) 18:593–603. doi: 10.1016/j.chom.2015.10.006

7. Su Xz, Zhang C, Joy DA. Host-malaria parasite interactions and impacts on mutual evolution. *Front Cell Infect Microbiol*. (2020) 10:587933. doi: 10.3389/fcimb.2020.587933

8. Yang X, Su Y, Li H, Zhuo X. Optimal control of a cell-to-cell fractional-order model with periodic immune response for HCV. *Symmetry*. (2021) 13:2121. doi: 10.3390/sym13112121

9. Sherling ES, van Ooij C. Host cell remodeling by pathogens: the exomembrane system in Plasmodium-infected erythrocytes. *FEMS Microbiol Rev*. (2016) 40:701–21. doi: 10.1093/femsre/fuw016

10. Mandala WL, Harawa V, Dzinjalamala F, Tembo D. The role of different components of the immune system against Plasmodium falciparum malaria: possible contribution towards malaria vaccine development. *Mol Biochem Parasitol*. (2021) 246:111425. doi: 10.1016/j.molbiopara.2021.111425

11. Engwerda CR, Good MF. Interactions between malaria parasites and the host immune system. *Curr Opin Immunol*. (2005) 17:381–7. doi: 10.1016/j.coi.2005.05.010

12. Greenwood BN, Marsh KS, Snow RW. Why do some African children develop severe malaria? *Parasitol Today*. (1991) 7:277–81. doi: 10.1016/0169-4758(91)90096-7

13. Baker DA. Malaria gametocytogenesis. *Mol Biochem Parasitol*. (2010) 172:57–65. doi: 10.1016/j.molbiopara.2010.03.019

14. McQueen PG, Williamson KC, McKenzie FE. Host immune constraints on malaria transmission: insights from population biology of within-host parasites. *Malar J*. (2013) 12:1–18. doi: 10.1186/1475-2875-12-206

15. Sreenivasamurthy SK, Dey G, Ramu M, Kumar M, Gupta MK, Mohanty AK, et al. A compendium of molecules involved in vector-pathogen interactions pertaining to malaria. *Malar J*. (2013) 12:1–7. doi: 10.1186/1475-2875-12-216

16. Acharya P, Garg M, Kumar P, Munjal A, Raja K. Host-parasite interactions in human malaria: clinical implications of basic research. *Front Microbiol*. (2017) 8:889. doi: 10.3389/fmicb.2017.00889

17. Pinheiro L, Feitosa LM, Silveira FF, Boechat N. Current antimalarial therapies and advances in the development of semi-synthetic artemisinin derivatives. *Anais Acad Brasil Ciências*. (2018) 90:1251–71. doi: 10.1590/0001-3765201820170830

18. Vera IM, Ruivo MTG, Rocha LFL, Marques S, Bhatia SN, Mota MM, et al. Targeting liver stage malaria with metformin. *JCI Insight*. (2019) 4:e127441. doi: 10.1172/jci.insight.127441

19. Bruce-Chwatt LJ. Classification of antimalarial drugs in relation to different stages in the life-cycle of the parasite: commentary on a diagram. *Bull World Health Organ*. (1962) 27:287.

20. Munro BA, McMorran BJ. Antimalarial drug strategies to target plasmodium gametocytes. *Parasitologia*. (2022) 2:101–24. doi: 10.3390/parasitologia2020011

21. Anvikar AR, Arora UR, Chattopadhya D, Das BC, Dash AP, Dhariwal A, et al. Guidelines for diagnosis and treatment of malaria in India. *Natl Inst Malaria Res*. (2011).

22. Organization WH. Guidelines for the Treatment of Malaria. Geneva: World Health Organization. (2015).

23. Anderson RM, May RM, Gupta CS. Non-linear phenomena in host-parasite interactions. *Parasitology*. (1989) 99:S59–79. doi: 10.1017/S0031182000083426

24. Hetzel CJ, Anderson RM. The within-host cellular dynamics of bloodstage malaria: theoretical and experimental studies. *Parasitology*. (1996) 113:25–38. doi: 10.1017/S0031182000066245

25. Elaiw A, Al Agha A. Global analysis of a reaction-diffusion within-host malaria infection model with adaptive immune response. *Mathematics*. (2020) 8:563. doi: 10.3390/math8040563

26. Li Y, Ruan S, Xiao D. The within-host dynamics of malaria infection with immune response. *Mathem Biosci Eng*. (2011) 8:999–1018. doi: 10.3934/mbe.2011.8.999

27. Anderson RM. Complex dynamic behaviours in the interaction between parasite populations and the host's immune system. *Int J Parasitol*. (1998) 28:551–66. doi: 10.1016/S0020-7519(97)00207-5

28. Song T, Wang C, Tian B. Mathematical models for within-host competition of malaria parasites. *Mathem Biosci Eng*. (2019) 16:6623–53. doi: 10.3934/mbe.2019330

29. Iggidr A, Kamgang JC, Sallet G, Tewa JJ. Global analysis of new malaria intrahost models with a competitive exclusion principle. *SIAM J Appl Math*. (2006) 67:260–78. doi: 10.1137/050643271

30. Tewa JJ, Fokouop R, Mewoli B, Bowong S. Mathematical analysis of a general class of ordinary differential equations coming from within-hosts models of malaria with immune effectors. *Appl Math Comput*. (2012) 218:7347–61. doi: 10.1016/j.amc.2011.10.085

31. Kamangira B, Nyamugure P, Magombedze G. A theoretical mathematical assessment of the effectiveness of coartemether in the treatment of Plasmodium falciparum malaria infection. *Math Biosci*. (2014) 256:28–41. doi: 10.1016/j.mbs.2014.07.010

32. Chen H, Wang W, Fu R, Luo J. Global analysis of a mathematical model on malaria with competitive strains and immune responses. *Appl Math Comput*. (2015) 259:132–52. doi: 10.1016/j.amc.2015.02.073

33. Khoury DS, Aogo R, Randriafanomezantsoa-Radohery G, McCaw JM, Simpson JA, McCarthy JS, et al. Within-host modeling of blood-stage malaria. *Immunol Rev*. (2018) 285:168–93. doi: 10.1111/imr.12697

34. Tabo Z, Luboobi LS, Ssebuliba J. Mathematical modelling of the in-host dynamics of malaria and the effects of treatment. *Parasitology*. (2000) 121:227–35. doi: 10.22436/jmcs.017.01.01

35. Chinebu TI, Ezennorom EO, Okwor JU. Simulation of an intracellular differential equation model of the dynamics of malaria with immune control and treatment. *Int J Trend Sci Res Dev*. (2018) 2:1–21. doi: 10.31142/ijtsrd18476

36. Orwa TO, Mbogo RW, Luboobi LS. Multiple-strain malaria infection and its impacts on plasmodium falciparum resistance to antimalarial therapy: a mathematical modelling perspective. *Comput Mathem Method Med*. (2019) 2019:9783986. doi: 10.1155/2019/9783986

37. Annan K. In-host analysis of malaria dynamics in humans. *Open J Appl Sci*. (2020) 10:191–209. doi: 10.4236/ojapps.2020.105015

38. Van den Driessche P, Watmough J. Reproduction numbers and sub-threshold endemic equilibria for compartmental models of disease transmission. *Math Biosci*. (2002) 180:29–48. doi: 10.1016/S0025-5564(02)00108-6

39. La Salle JP. *The Stability of Dynamical Systems*. Philadelphia, PA: SIAM. (1976). doi: 10.1137/1.9781611970432

40. Orwa T, Mbogo R, Luboobi L. Mathematical model for the in-host malaria dynamics subject to malaria vaccines. *Lett Biomathem*. (2018) 5:222–51. doi: 10.1080/23737867.2018.1526132

41. Selemani MA, Luboobi LS, Nkansah-Gyekye Y. On stability of the in-human host and in-mosquito dynamics of malaria parasite. *Asian J Mathem Appl*. (2016) 2016:1–23.

42. Anderson RM, May RM. *Infectious Diseases of Humans*. Oxford UK: Oxford University Press. (1991). doi: 10.1093/oso/9780198545996.001.0001

43. Selemani MA, Luboobi LS, Nkansah-Gyekye Y. The in-human host and in-mosquito dynamics of malaria parasites with immune responses. *New Trends Mathem Sci*. (2017) 5:182–207. doi: 10.20852/ntmsci.2017.196

44. Hellriegel B. Modelling the immune response to malaria with ecological concepts: short-term behaviour against long-term equilibrium. *Proc R Soc London B*. (1992) 250:249–56. doi: 10.1098/rspb.1992.0156

45. Chiyaka C, Garira W, Dube S. Modelling immune response and drug therapy in human malaria infection. *Comput Math Methods Med*. (2008) 9:143–63. doi: 10.1080/17486700701865661